Advances in Science and Technology Research Journal, 2025, 19(12), 56–66 https://doi.org/10.12913/22998624/209706 ISSN 2299-8624, License CC-BY 4.0

Influence of cooling medium on mechanical properties of AA7075-T651 submerged friction stir welded joints

Robert Kosturek^{1*}, Janusz Torzewski¹, Daniel Klápště², Jaromír Moravec²

- ¹ Department of Fatigue and Machine Design, Faculty of Mechanical Engineering, Military University of Technology, gen. S. Kaliskiego 2 Str., Warsaw, Poland
- ² Department of Engineering Technology, Faculty of Mechanical Engineering, Technical University of Liberec, Studentská 1402/2 Str., Liberec, Czech Republic
- * Corresponding author's e-mail: robert.kosturek@wat.edu.pl

ABSTRACT

This study explores the influence of various conventional cooling media (water, cutting fluid, and quenching oil) on the mechanical properties of in AA7075-T61 aluminum alloy FSW joints. Cooling media had minimal impact on the macrostructure of AA7075-T651 joints, though a slight increase in the amount of dynamically recrystalized grains was observed in the upper part of the weld. A 5–10% increase in LHZ hardness (up to 131 HV0.1) was achieved, and the HAZ width was reduced from 15 mm to 11 mm, with water-based cooling showing the best results. The use of different cooling media improved joint strength, with joint efficiency reaching up to 85.3% for a 10% Blasocut 2000 solution. The results also indicated a direct relationship between the heat absorbed by the cooling media and the ultimate tensile strength of the joints. Although FSW joints enhanced strain-hardening capacity, external cooling slightly reduced this effect, with H values decreasing from 0.414 to 0.380.

Keywords: friction stir welding, mechanical properties, underwater welding, cooling, quenching oil, cutting fluid.

INTRODUCTION

The friction stir welding (FSW) technique is currently one of the most effective methods for manufacturing solid-state joints in 2XXX, 6XXX and 7XXX series aluminum alloys. In recent years, many studies have focused on optimizing FSW parameters for precipitation-hardened aluminum alloys, particularly from the 6XXX series, aiming to maximize tensile strength and microhardness by controlling tool rotational speed, welding velocity, and axial load [1]. For dissimilar joints between AA6XXX and AA5XXX alloys, research highlights that proper parameter selection is crucial to avoid defects and limit the formation of brittle intermetallic compounds such as Al₃Mg₂, whose presence has been correlated with a drop in ductility of over 30% and a tensile strength reduction from ~160 MPa to below 120 MPa [2]. Investigations on high-strength alloys such as EN AW-2024-T3 show that even small deviations in tool trajectory can disturb material flow, reduce weld homogeneity, and lower load capacity, which makes multi-criteria optimization necessary to ensure both mechanical performance and process stability [3].

Received: 2025.07.20

Accepted: 2025.10.01

Published: 2025.11.01

Recently, a variant of FSW method that has been gaining increasing popularity is UWFSW (underwater friction stir welding), which incorporates external water cooling during the welding operation [4, 5]. This approach has demonstrated significant improvements in the mechanical properties and microstructural integrity of joints in aluminum alloys, particularly those in precipitationhardened aluminum alloys [4, 6–8]. For the water environment drastically reduces the peak temperature and accelerates the cooling rate during welding, it inhibits grain growth and limits the dissolution and coarsening of strengthening precipitates in the heat-affected zone (HAZ) and thermo-mechanically affected zone (TMAZ), which are typically the weakest regions in standard FSW joints [9]. Microstructural analysis reveals that UWFSW joints exhibit finer, equiaxed grains in the stir zone (SZ) due to dynamic recrystallization, while the narrower softened zone and suppressed grain growth lead to increased hardness in the TMAZ and HAZ compared to air-cooled FSW joints [6]. TEM studies further confirm that UWFSW helps preserve or re-precipitate fine strengthening phases (e.g., MgZn, or θ') which are often lost in conventional FSW due to excessive heat [7]. For this reason, UWFSW joints consistently outperform their FSW counterparts in tensile strength, joint efficiency, and sometimes elongation. For example, joints in AA2519-T87 [8] and AA7075 [10, 11] alloys showed increases in tensile strength of up to 20% under optimized UWFSW parameters. UWF-SW joints of precipitation-hardened aluminum alloys are also characterized by improved fatigue strength, including in the low-cycle fatigue regime [12, 13], with recent research findings further suggesting that they exhibit greater predictability of fatigue lifetime within the LCF range [14].

In addition to the positive effects on improving mechanical properties, research on welding in underwater environments also has significant practical relevance, particularly in the context of joining aluminum alloys used in marine engineering [15,16]. Some studies report that UWFSW is an effective method for in-situ repair of marine structures in wet docks, made of AA5754 [15] and AA5083 alloys [16] due to its solid-state nature that eliminates fusion-related defects and the need for shielding gas.

Recently, due to the use of cooling media other than water for performing FSW joints, including liquid nitrogen (cryogenic friction stir welding - CFSW) [17] and solid carbon dioxide-based liquid mixtures [18], the term submerged friction stir welding (SFSW) has been adopted for all processes carried out in a cooling medium. It should be noted that the use of liquid medium for cooling is not equivalent to the SFSW process, as e.g. liquid nitrogen may be merely poured onto the joint after the tool has passed, without full immersion of the joined elements (rapid cooling friction stir welding - RCFSW) [19, 20]. In the context of UWFSW joints, it is worth citing the study conducted by Wakchaure et al., who investigated the effect of initial water temperature on the properties of UWFSW joints in 6 mm AA6061-T6 alloy plates, demonstrating that hot water (80 °C) enabled the production of joints with the highest UTS value (over 248 MPa) and greater ductility

compared to joints produced under conventional air cooling conditions [21].

The literature consistently confirms a significant improvement in the mechanical properties of FSW joints in 2XXX, 6XXX and 7XXX series aluminum alloys when welded under underwater conditions. Nevertheless, a research gap still exists regarding the specific influence of individual cooling media on the mechanical performance of such joints. For example, in the authors' previous studies [13], as well as in other limited literature sources [10], it has been shown that using a cutting fluid solution instead of water can enhance the ductility of the joints and improve certain strength-related parameters of the AA7075 alloy, including ultimate tensile strength.

The aim of this study was to investigate how different cooling media, commonly used in the metal industry, affect the mechanical properties of FSW joints in AA7075-T61 alloy. In this context, the present article serves as an extension of previous research on FSW joining of this alloy in a water environment [13]. Despite the undeniable advantages of performing FSW under cryogenic conditions, we chose to use conventional cooling media such as water, cutting fluid at various concentrations, and quenching oil. This decision was driven by the intent to maintain the cleanliness and safety of the FSW technique; among other reasons, due to the harmfulness of vapors to the operator, we limited our selection to these commonly used and industry-accepted media.

MATERIALS AND METHODS

The subject of the study was friction stir welded joints of AA7075-T651 aluminum alloy in the form of 5 mm thick sheets. The mechanical properties and chemical composition of the alloy are presented in Tables 1 and 2, respectively. Chemical composition (Table 1) was provided by the manufacturer, Bikar Metalle GmbH, while mechanical properties (Table 2) are the result of the authors' own investigations.

The sheets were cut into strips measuring 500 × 80 mm. Welding was performed along the longer edge of the strips, transverse to the rolling direction. Prior to welding, the edges of the sheets were milled, the top surfaces were abraded with sandpaper, and subsequently degreased with isopropanol. The joining process was carried out using an ESAB Legio 4UT machine, equipped with

Table 1. Chemical composition of AA7075-T651 alloy (% weight)

			İ				1		
	Si	Fe	Cu	Mn	Mg	Cr	Zn	Ti	Al
-	0.071	0.122	1.610	0.025	2.596	0.197	5.689	0.041	Base

Table 2. Mechanical properties of AA7075-T651 alloy

Yield strength, YS	Tensile strength, UTS	Elongation at break, A	Microhardness	
532.3 ± 2.7 MPa	584.9 ± 0.9 MPa	14.3 ± 0.4 %	167.5 ± 5.6 HV0.1	

an ESAB tool (catalogue no. 0810134-001). All welds were produced under identical process parameters: a tool rotational speed of 600 rpm, welding speed of 125 mm/min, tool tilt angle of 2°, and a plunge depth of 4.8 mm. This set of parameters is the result of previous research on UWFSW joints of the AA7075-T651 alloy conducted by the authors [13]. The total length of each individual weld was 480 mm. In total, five different joints were fabricated: one reference FSW joint cooled in air, and four submerged joints welded under different cooling media. An overview of all sample variants is provided in Table 3.

For the SFSW process, the tank was filled so that the liquid level was 20 mm above the upper surface of the sheets. An example image of the experimental setup used is shown in Figure 1.

To estimate the heat absorbed by the cooling media, the liquid temperature was measured before and after welding using a DT-2 digital thermometer. After welding, samples were extracted from the joints for microstructural examination and static tensile testing. Specimens for microstructural analysis were sectioned from the welded plates and subsequently prepared using standard metallographic techniques. This

Table 3. Cooling media and sample designations

Sample designation	Description / cooling medium		
Air	Air-cooled, conventional friction stir welding		
OH-70	OH-70 quenching oil, provided by ATN Oleje Tap water		
Water			
5% CF	4.8% solution of Blasocut 2000 in water		
10% CF	9.8% solution of Blasocut 2000 in water		

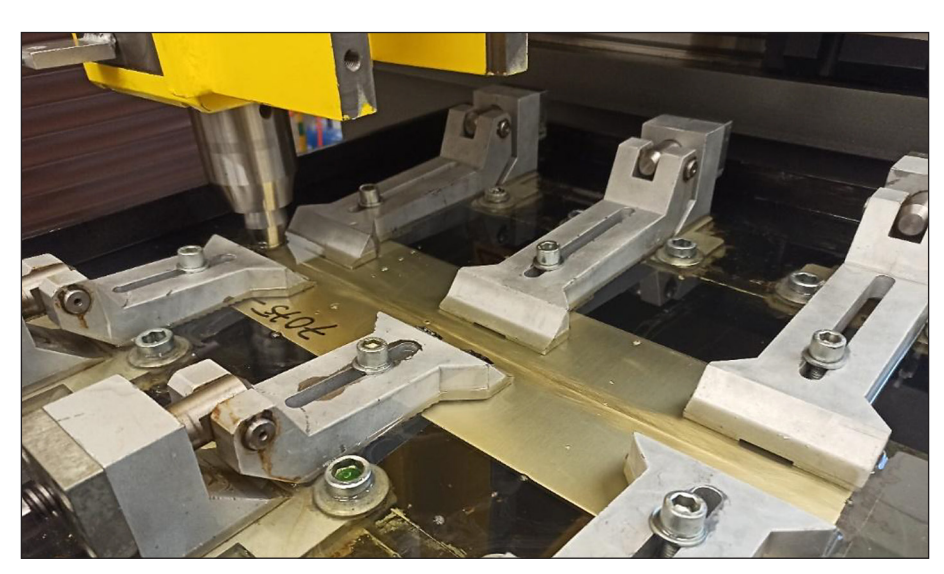


Figure 1. The welding setup shown using quenching oil as the cooling medium

involved embedding the samples in resin, followed by grinding, polishing, and chemical etching. Keller's reagent was used as the etchant, composed of 20 ml distilled water, 5 ml of 63% nitric acid (HNO₃), 1 ml of 40% hydrofluoric acid (HF), and two drops of 36% hydrochloric acid (HCl), with an etching duration of approximately 10 s. Macrostructural observations were performed using an OLYMPUS LEXT OLS4100 microscope. The fabricated joints were further examined for their microhardness profiles using a Struers DURA SCAN 70 hardness tester. A load of 0.98 N was applied for 10 s during each measurement. Microhardness was measured along the cross-section of each weld at mid-thickness (2.5 mm below the upper surface of the welded plates). To assess the mechanical properties of the joints, tensile tests were conducted on an IN-STRON 8802 MTL universal testing machine, following the ASTM E8/E8M-13a standard [22]. The geometry of the tensile sample is illustrated in Figure 2. All error bars presented in this paper refer to the standard deviation.

RESULTS AND DISCUSSION

Temperature measurements

In the first stage of the study, temperature measurements of the cooling media were carried out before and after the welding process in order to estimate the heat absorbed during the formation of the joint over a length of 480 mm. The data

necessary for calculating heat capacity: density and specific heat, were compiled based on literature sources and are presented in Table 4.

It should be emphasized that, as these values are not derived from direct measurements, they are subject to a certain degree of inaccuracy. Therefore, the subsequently reported values of absorbed heat should be regarded as estimates of the actual values. The quantity of heat absorbed by a cooling medium was determined using the following equation:

$$Q = mc\Delta T \tag{1}$$

where: m – the mass of the substance [kg], c – the specific heat of the substance [kJ/kg×K], Δ T - the change in temperature [K].

The results of the temperature measurements and the estimated absorbed heat are presented in Table 5. Based on the obtained results, it can be concluded that the cutting fluid solutions absorbed the most heat, which is also confirmed by the tensile test results discussed later in this publication. A comparison of the estimated heat absorption for all cooling media is shown in Figure 3.

An important observation is that, despite its lower specific heat, the Blasocut 2000 solution absorbed more heat than pure water during the welding process. This can be attributed primarily to its improved surface wettability and more favorable evaporation behavior. As an emulsion, the Blasocut solution spreads more effectively over the hot metal surface, increasing the actual contact area

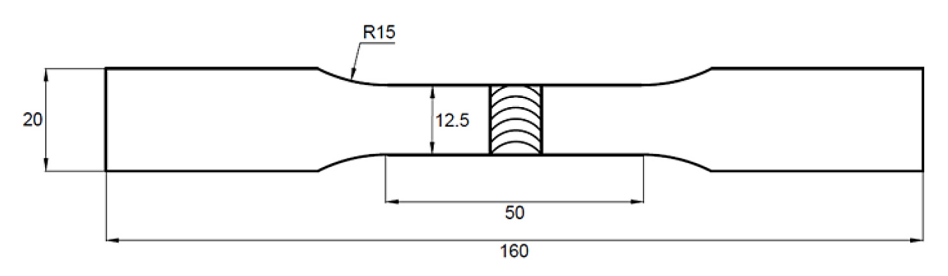


Figure 2. Schematic of the tensile test sample

Table 4. Selected physical properties of applied cooling media

Cooling medium	Temperature range [°C]	Specific heat [kJ / kg × K]	Density [kg / m³]	Mass [kg]	Heat capacity [kJ / K]
OH-70	20–30	1.91	858.00	9.87	18.9
Water	20–25	4.18	997.63	11.47	48.0
5% CF	20–25	4.07	995.30	11.45	46.6
10% CF	20–30	3.96	992.17	11.41	45.2

Table 5. Results of temperature measurements and the absorbed heat

Si	Fe	Cu	Mn	Mg	Cr	Zn	Ti	Al
0.071	0.122	1.610	0.025	2.596	0.197	5.689	0.041	Base

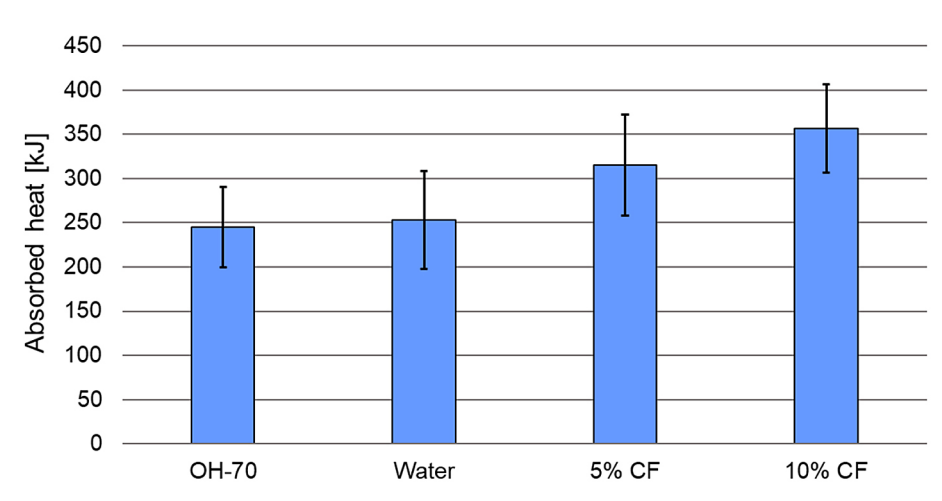


Figure 3. Heat absorbed by the investigated cooling media

and enhancing convective heat transfer [23]. Additionally, unlike water, which can rapidly vaporize and form an insulating steam layer, as observed by the authors in the UWFSW process, the emulsion evaporates more gradually, allowing sustained thermal contact and more consistent cooling [24]. These effects combine to yield higher effective heat absorption, not due to a higher heat capacity, but rather through more efficient interfacial heat transfer and improved thermal stability.

Microstructure

The structural analysis included macrostructure observations and grain size measurements in the stir zone. Images of selected macrostructures are shown in Figure 4.

In the previous study, no effect of performing the FSW process underwater on the joint

macrostructure was observed [13]. Similarly, in this case, no significant influence of the cooling media on the macrostructure is observed. All joints are free from imperfections, and the applied welding speed of 125 mm/min ensures complete material mixing regardless of the cooling media used. The only area that distinguishes the conventionally produced joint (in air) is the upper region of the thermo-mechanically affected zone on the advancing side (indicated by the red circle in Figure 4a). In this area, a lower fraction of dynamically recrystallized grains is observed, with a higher presence of deformed grains compared to the joints produced in cooling media (Figure 4b-d). It should be noted that although FSW joints generally exhibit high repeatability, further studies of the thermo-mechanically affected zone are necessary to clearly explain the cause

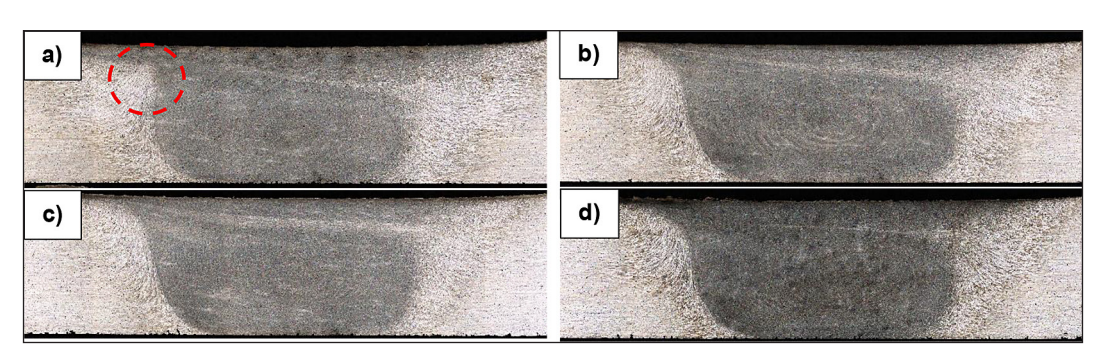


Figure 4. Macrostructures of samples: air (a), OH-70 (b), water (c) and 10% CF (d)

of the observed difference. More pronounced differences between the samples were observed by Sabari et al. in the welding of AA2519-T87 under normal and underwater conditions [25]. These differences included, among others, variations in the fraction of dynamically recrystallized regions. The differences reported in their study for joints produced at 1300 rpm [25] are consistent with the larger dynamically recrystallized zone observed in the SFSW joints presented in the current study (Figure 4a,b). Some research studies report a significant influence of additional cooling on the grain size in the stir zone (mainly referring to RCFSW processes), enabling, for example in the case of magnesium alloys, an almost tenfold grain refinement compared to the conventional FSW process [26]. Although from the perspective of joint performance, grain refinement does not play a major role — as failure still occurs in the low-hardness zone (LHZ) — it was decided to investigate the influence of the applied cooling media on the grain size in the stir zone. The measurements were taken at different distances from the top surface of the welded plates: 0.5 mm (top), 2.5 mm (center), and 4.5 mm (bottom), and the obtained results are summarized in Table 6.

Analysis of the grain size measurement results indicates that, in the case of the conventional FSW joint, the average grain size is approximately 2.5 μm, regardless of the distance from the top surface of the welded plates. The joints produced in different cooling media exhibit relatively significant variation in results, both in terms of average grain size and the 95th percentile. The data suggest that the joints produced in water and quenching oil are characterized by the finest grain size; however, considering the spread of the results, it would be more appropriate to state that the ability to draw clear conclusions is considerably limited. In fact, based on the 95th percentile, the finest grain is generally observed in the upper and lower regions of the weld nugget in most cases. It can generally be assumed that the average grain size in the weld nugget of the analyzed SFSW joints falls within the range of approximately 1.7 to 3 µm and does not appear to differ significantly from the average values observed in conventionally welded joints. Therefore, in the examined regions, no substantial grain refinement is observed, as is the case in RCFSW processes [27].

Microhardness

The obtained microhardness distributions of the examined FSW joints are presented below in Figure 5. A characteristic "W"-shaped profile, typical of FSW joints in precipitation-hardened aluminum alloys, is observed. Regardless of the cooling media used, the microhardness distribution follows the same general pattern, differing only in the width of the HAZ and the microhardness values within the low-hardness region. In the case of the conventional FSW joint performed in air, the LHZ is located approximately 11 mm from the weld center and is characterized by a microhardness of about 119-121 HV0.1. In reference to literature data, it can be concluded that the obtained hardness in the LHZ is relatively high. In most other studies, reported values typically range from 80-90 HV0.1 [27], 90 HV0.1 [28], to 105 HV0.1 [29], depending on the thickness of the components and the applied welding process parameters. However, the value presented in the current study is consistent with the authors' previous research on the welding of 5 mm thick AA7075-T651 sheets, where, across a wide range of welding parameters, the hardness in the LHZ ranged from 110 to 120 HV0.1 [30]. Taking the conventionally produced joint as a reference point, it is also worth noting that the width of the HAZ extends up to 15 mm from the weld center. In all cases, the use of additional cooling resulted in a narrower HAZ and an increase in hardness within the LHZ. The

Table 6. Results of grain size measurements in the stir zone (in μm)

	Bot	tom	Cer	nter	Тор		
Sample	Average grain size	The 95 th percentile	Average grain size	The 95 th percentile	Average grain size	The 95 th percentile	
Air	2.56	6.81	2.47	6.36	2.64	7.12	
OH-70	2.05	5.23	1.93	5.58	1.72	4.36	
Water	1.81	4.76	2.23	6.03	1.91	4.67	
5% CF	3.00	8.27	3.15	9.18	2.66	8.20	
10% CF	2.41	7.49	2.29	4.76	2.44	7.20	

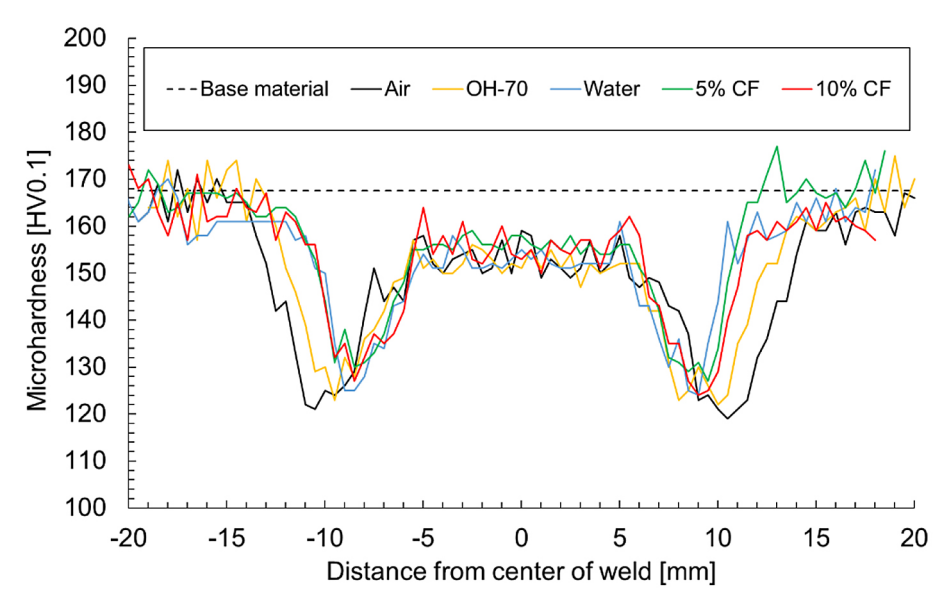


Figure 5. Microhardness distributions of the examined welded joints

weakest effect was observed with the use of OH-70 quenching oil, which yielded an SFSW joint with the LHZ hardness of 122-123 HV0.1 and the HAZ extending up to 13-14 mm from the weld center. The narrowing of the HAZ is more clearly observed in the case of water-based cooling media. The recorded LHZ hardness values are 124-125 HV0.1, 127-131 HV0.1, and 124-127 HV0.1 for the Water, 5% CF, and 10% CF samples, respectively. It should be noted that the spacing between indentations during the microhardness test was 0.5 mm; therefore, it cannot be confirmed with certainty that the measurements captured the softest region. For this reason, the reported ranges reflect the lowest recorded values on both the advancing and retreating sides. When compared to the conventional joint, the measured values indicate a 5-6% increase in LHZ hardness, along with a reduction in HAZ width to 11-12 mm from the weld center for all water-based media. It is worth noting that the increase in LHZ hardness observed in this study is solely attributable to the type of cooling media used. Its hardness can be further significantly increased by raising the welding speed, as demonstrated in the authors' previous study on UWF-SW [13]. Moreover, the literature on UWFSW of AA7075 includes reports of LHZ hardness values exceeding 140 HV0.1 [11]. The increases in LHZ hardness presented in this study are, in percentage terms, consistent with the data reported in the study on the effect of cutting fluid and liquid nitrogen cooling on the properties of FSW joints in 4 mm thick AA7075 alloy sheets [10].

Literature reports on increased microhardness in the stir zone as a result of underwater welding conditions [11] cannot be clearly confirmed for the joints analyzed in this study. The obtained SZ hardness values (Figure 5) for all samples generally range between 150–160 HV0.1, and the grain size analysis (Table 6) likewise does not provide a basis for such a conclusion.

Tensile properties

To determine the basic mechanical properties of the fabricated joints, static tensile tests were carried out. Representative stress—strain curves are shown in Figure 6, while the recorded values of yield strength (YS) and ultimate tensile strength (UTS), along with standard deviations, are presented in Figure 7.

The general shape of the tensile curves is similar for all FSW joints, with the main differences observed in the YS and ultimate tensile strength values. As is typical for FSW joints in AA7075 alloy, a significant reduction in the yield strength of the base material is observed, along with a decrease in UTS and ductility (Figure 6). Primarily due to the lowered YS, AA7075 FSW joints exhibit a higher capacity for plastic deformation before reaching UTS, which will be discussed later in this paper.

In general, a decrease in YS is observed from approximately 530 MPa to 320 MPa (Air), 335 MPa (OH-70), and around 355 MPa (Water, 5% CF, 10% CF). Depending on the cooling media used, this represents a reduction of

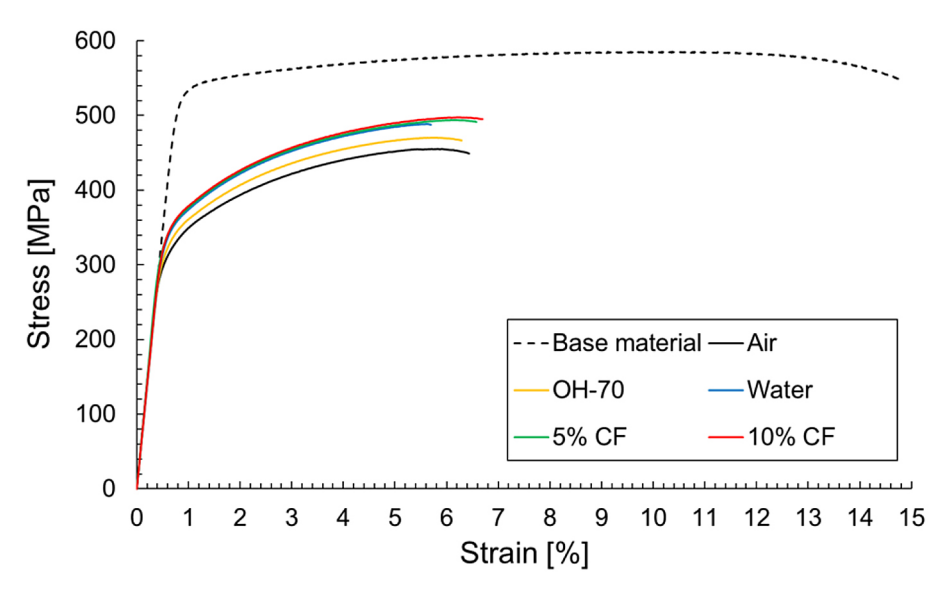


Figure 6. Representative tensile curves of the examined welded joints

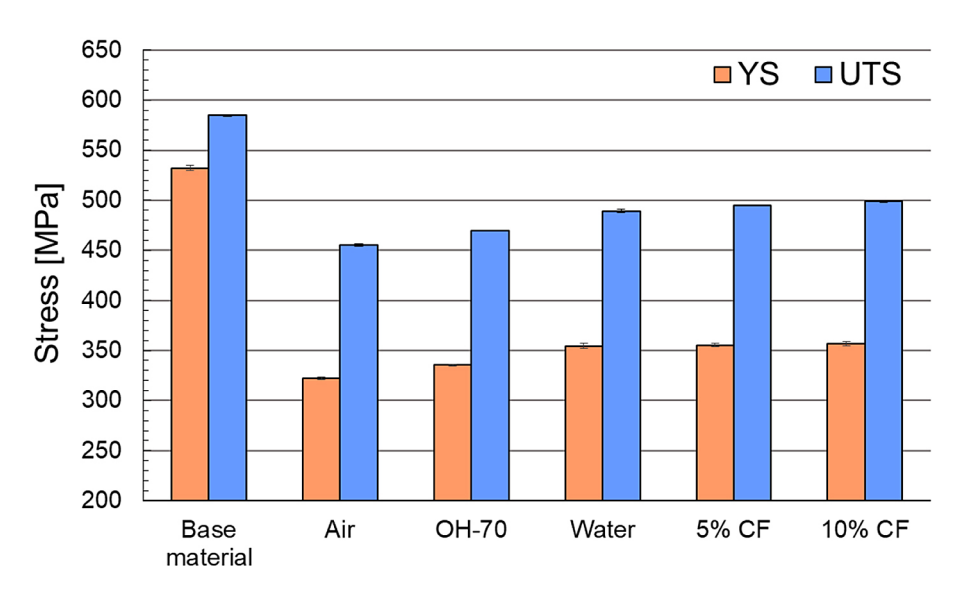


Figure 7. Mean values of selected strength parameters for the examined welded joints

approximately 35–40%. Slightly smaller reductions are seen in UTS, where the base material value of about 585 MPa decreases to 455 MPa (Air), 470 MPa (OH-70), 490 MPa (Water), 495 MPa (5% CF), and slightly below 500 MPa (10% CF). A clear correlation can therefore be observed between the heat absorbed during the joining process (Figure 3) and the tensile strength of the resulting joint (Figure 7). The differences between YS and UTS values result in varying susceptibility to plastic deformation before reaching UTS, which can be expressed using the strain hardening capacity parameter, defined by the following formulas (two variants) [31]:

$$H_c = \frac{\sigma_{UTS} - \sigma_{YS}}{\sigma_{YS}} = \frac{\sigma_{UTS}}{\sigma_{YS}} - 1 \tag{2}$$

The calculated values of strain hardening capacity, joint efficiency, and other mechanical parameters of the tested samples are summarized in Table 7. As already observed in Figure 6, a decrease in ductility can be seen in the FSW joints, reflected in the lower elongation at fracture (A) values. This reduction is fairly consistent across all joints, amounting to over 50%. The only notable exception is the 'Water' sample, which shows the lowest elongation at break values, dropping below 6%. An important observation is that the analyzed FSW and UWFSW joints exhibit relatively low variability in the measured

Sample	YS [MPa]	UTS [MPa]	A [%]	Hc	Joint efficiency				
Base material	532.3 ± 2.7	584.9 ± 0.9	14.3 ± 0.4	0.099	-				
Air	322.1 ± 1.4	455.4 ± 1.0	6.3 ± 0.2	0.414	77.9%				
OH-70	335.4 ± 0.6	469.7 ± 0.5	6.3 ± 0.2	0.401	80.3%				
Water	354.7 ± 2.8	489.4 ± 1.8	5.6 ± 0.2	0.380	83.7%				
5% CF	355.4 ± 1.5	494.7 ± 0.6	6.7 ± 0.2	0.392	84.6%				
10% CF	357 1 + 2 1	498 8 + 0 9	67+01	0.397	85.3%				

Table 7. Selected mechanical properties of the examined welded joints

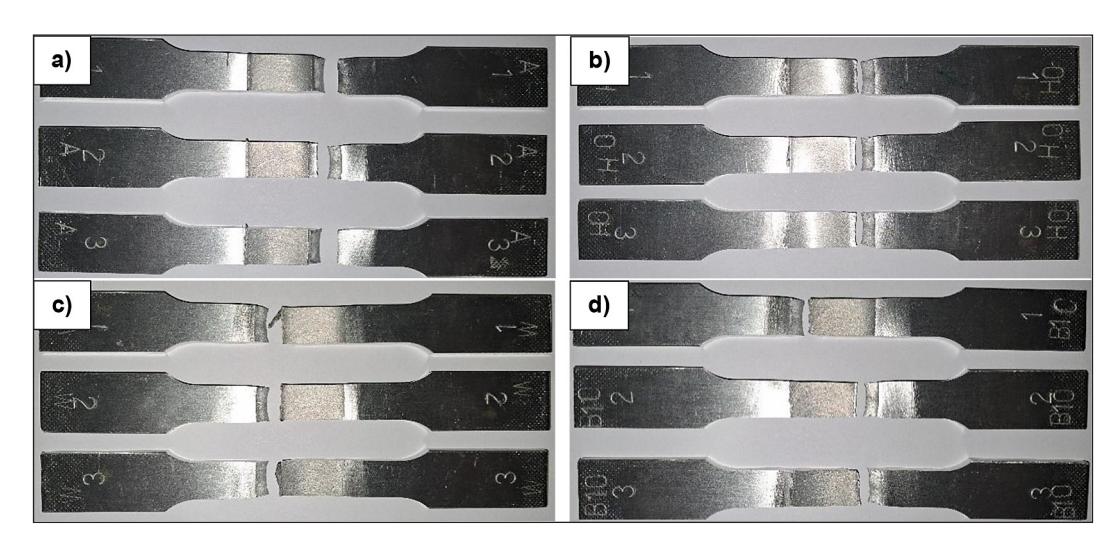


Figure 8. Selected fractured samples: air (a), OH (b), water (c), and 10% CF (d)

mechanical parameters, as reflected by the calculated standard deviation values. Joint efficiency increases with the heat absorbed by the cooling media, ranging from 77.9% (Air) to the highest value of 85.3% for 10% CF. These values should be compared to the results obtained in a previous study [13], where the highest efficiency of 89% was achieved for a water-cooled SFSW joint. That result corresponded to a sample welded at a higher welding speed (150 mm/min) and tool rotational speed (800 rpm), which also exhibited the highest LHZ hardness value (approximately 131-136 HV0.1) [13]. An increase in the hardness of the LHZ in UWFSW joints of AA7075 alloy as a result of higher tool rotational speed has been reported in the literature [11]. However, the primary parameter determining joint strength remains the welding speed [6,13].

Analysis of the strain hardening capacity results indicates that the FSW process itself leads to a significant increase in this parameter – more than fourfold. The extent of this increase depends on the process parameters and the specific material, but for precipitation-hardened

aluminum alloys, such values are reported in the literature [31]. The application of a cooling medium results in a noticeable reduction in strain-hardening capacity, and an inverse correlation is evident between the heat absorbed during welding and the value of this parameter. Nevertheless, regardless of the cooling conditions used and the resulting differences in joint characteristics, none of the FSW samples achieved strain-hardening capacity values that come close to those of the base material, highlighting a general limitation of the process in preserving this particular mechanical property. Images of selected fractured tensile samples are presented below (Figure 8).

In all analyzed samples, failure occurred at the boundary between the TMAZ and HAZ, which corresponds to the LHZ identified in this study. Fractures were observed on the retreating side (Figure 8a, b), the advancing side (Figure 8c), and, in some cases, randomly within either zone (Figure 8d). Importantly, no fractures were recorded within the SZ itself, indicating the high quality of the manufactured joints.

CONCLUSIONS

The conducted research leads to the following conclusions:

- 1. The applied cooling media had no significant effect on the macrostructure of the joints, although a slightly higher fraction of dynamically recrystallized grains was observed in the upper part of the joints on the advancing side of cooled samples, and grain size measurements in the stir zone confirmed only minor variations regardless of the cooling method.
- 2. The use of different cooling media in the FSW process of AA7075-T651 alloy resulted in a 5–10% increase in LHZ hardness (up to 131 HV0.1) and a reduction in HAZ width from 15 mm to 11 mm, with the most effective improvement observed for water-based cooling with cutting fluid.
- 3. The application of different cooling media during FSW of AA7075 significantly influences joint strength, with increased heat removal leading to higher yield strength and joint efficiency, reaching up to 85.3% for the 10% Blasocut 2000 solution. A relationship is observed between the UTS of the joint and the heat absorbed by a cooling media during the welding process.
- 4. The FSW process significantly enhances the strain-hardening capacity of the AA7075-T651 alloy compared to the base material; however, this effect is slightly reduced with the use of external cooling, as indicated by a gradual decrease in Hc values from 0.414 (conventional FSW) to 0.380 (SFSW with tap water cooling).

Acknowledgements

This work was financed by Military University of Technology under research project UGB 22-015/2025.

REFERENCES

- Jamaludeen U.M. Examination and optimization of friction stir welding process parameters of AA6092 alloys. Soldagem & Inspeção, 2024, 29, e2907. https://doi.org/10.1590/0104-9224/SI29.07
- Osorio Díaz M.A., Franco Arenas A., Unfried-Silgado, J. Effects of process parameters on mechanical properties and microstructure of AA6063-T6 and AA5052-H32 dissimilar friction stir welded joints.

- Soldagem & Inspeção, 2024, 29, e2911. https://doi.org/10.1590/0104-9224/SI29.11
- Bucior M., Kluz R., Kubit A., Aghajani D.H., Cestino E., Slota J. Friction stir welding tool trajectory error on the load capacity of EN AW-2024-T3 aluminum alloy joints. Journal of Advanced Joining Processes 2025, 12, 100325. https://doi.org/10.1016/j.jajp.2025.100325
- 4. Saravana Sundar A., Radhika N., Kumar A. Role of submerged friction stir welding in reducing intermetallic growth and enhancing microstructure in dissimilar Al–Ti joints. Sci Rep. 2024, 14, 26908. https://doi.org/10.1038/s41598-024-78130-x
- Memon S., Tomków J., Derazkola H.A. Thermo-mechanical simulation of underwater friction stir welding of low carbon steel. Materials 2021, 14, 17, 4953. https://doi.org/10.3390/ma14174953
- Liu H.J., Zhang H.J., Yu L. Effect of welding speed on microstructures and mechanical properties of underwater friction stir welded 2219 aluminum alloy. Materials and Design 2011, 32, 4, 1548–1553. https://doi.org/10.1016/j.matdes.2010.09.032
- Bijanrostami K, Vatankhah Barenji R. Underwater dissimilar friction stir welding of aluminum alloys: Elucidating the grain size and hardness of the joints. Proc Inst Mech Eng L J Mater Des Appl. 2019, 233, 4, 763–775. https://doi.org/10..1177/1464420716686625
- 8. Sabari S., Malarvizhi S., Balasubramanian V. Influences of tool traverse speed on tensile properties of air cooled and water cooled friction stir welded AA2519-T87 aluminium alloy joints. Journal of Materials Processing Technology 2016, 237. https://doi.org/10.1016/j.jmatprotec.2016.06.015
- Kosturek R., Torzewski J., Joska Z., Wachowski M., Śnieżek L. The influence of tool rotation speed on the low-cycle fatigue behavior of AA2519-T62 friction stir welded butt joints. Engineering Failure Analysis 2022, 142, 106756. https://doi. org/10.1016/j.engfailanal.2022.106756
- Saeyang P., Chanpariyavatevong A., Lamkham K., Siwadamrongpong S., Tantrairatn S. Influence of cooling methods in friction stir welding of 7075 aluminum alloy. International Journal of Engineering Research in Mechanical and Civil Engineering 2023, 10, 4. https://doi.org/01.1617/vol10/iss4/pid18053
- Rouzbehani R., Kokabi A.H., Sabet H., Paidar M., Ojo O.O. Metallurgical and mechanical properties of underwater friction stir welds of Al7075 aluminum alloy. Journal of Materials Processing Technology 2018, 262, 239–256. https://doi.org/10.1016/j. jmatprotec.2018.06.033
- 12. Xu W.F., Liu J.H., Chen D.L., Luan G.H. Lowcycle fatigue of a friction stir welded 2219-T62 aluminum alloy at different welding parameters and cooling conditions. Int J Adv Manuf

- Technol 2014, 74, 209–218. https://doi.org/10.1007/s00170-014-5988-z
- Kosturek R., Torzewski J., Śnieżek L. Study on Underwater Friction Stir Welding of AA7075-T651. Advances in Science and Technology Research Journal. 2024, 18, 8, 191–203. https://doi. org/10.12913/22998624/193529
- Kosturek R., Ślęzak T., Torzewski J. Structural Integrity of AA7075-T651 UWFSW Joints. Advances in Materials Science, 2024, 24, 4, 98–110. https://doi.org/10.2478/adms-2024-0025
- Janeczek A., Tomków J., Derazkola H.A., Fydrych D. Effect of underwater friction stir welding parameters on AA5754 alloy joints: experimental studies. Int J Adv Manuf Technol 2024, 134, 5643–5655. https://doi.org/10.1007/s00170-024-14485-9
- Saravanakumar R., Rajasekaran T., Pandey C. Underwater friction stir welded armour grade AA5083 aluminum alloys: experimental ballistic performance and corrosion investigation. J. of Materi Eng and Perform 2023, 32, 10175–10190. https://doi.org/10.1007/s11665-023-07836-2
- 17. Mofid M.A., Abdollah-Zadeh A., Ghaini F.M. Gür C.H. Submerged friction-stir welding (SFSW) underwater and under liquid nitrogen: an improved method to join Al alloys to Mg alloys. Metall Mater Trans A 2012, 43, 5106–5114. https://doi.org/10.1007/s11661-012-1314-2
- 18. Khodabakhshi F., Gerlich A.P., Simchi A., Kokabi A.H. Cryogenic friction-stir processing of ultrafine-grained Al–Mg–TiO2 nanocomposites. Materials Science and Engineering: A 2015, 620, 471–482. https://doi.org/10.1016/j.msea.2014.10.048
- 19. Trojovský P., Dhasarathan V., Boopathi S. Experimental investigations on cryogenic friction-stir welding of similar ZE42 magnesium alloys. Alexandria Engineering Journal 2023, 66, 1–14. https://doi.org/10.1016/j.aej.2022.12.007
- 20. Xu N., Qiu Z., Ren Z., Shen J., Wang D., Song Q., Zhao J., Jiang Y., Bao Y. Enhanced strength and ductility of rapid cooling friction stir welded ultralight Mg–14Li–1Al alloy joint. Journal of Materials Research and Technology, 2023, 23, 4444–4453. https://doi.org/10.1016/j.jmrt.2023.02.083
- 21. Wakchaure K., Chaudhari R., Thakur A., Fuse K., Lopez de Lacalle L.N., Vora J. The effect of cooling temperature on microstructure and mechanical properties of Al 6061-T6 aluminum alloy during submerged friction stir welding. Metals, 2023, 13, 7, 1159. https://doi.org/10.3390/met13071159
- 22. Standard Test Methods for Tension Testing of

- Metallic Materials. ASTM E8/E8M–13a, ASTM International, 2013.
- 23. Singh G., Khanna R., Dogra M. Spreadability studies of metal working fluids on tool surface and its impact on minimum quantity cooling and lubrication in turning. J Mater Process Technol, 2017, 243, 365–378. https://doi.org/10.1016/j.jmatprotec.2016.12.020
- 24. Pape F., Nassef B.G, Schmölzer S., Stobitzer D., Taubmann R., Rummel F., Stegmann J., Gerke M., Marian M., Poll G., Kabelac S. Comprehensive evaluation of the rheological, tribological, and thermal behavior of cutting oil and water-based metalworking fluids. Lubricants, 2025, 13(5), 219. https:// doi.org/10.3390/lubricants13050219
- 25. Sree Sabari S., Malarvizhi S., Balasubramanian V. Characteristics of FSW and UWFSW joints of AA2519-T87 aluminium alloy: Effect of tool rotation speed. Journal of Manufacturing Processes 2016, 22, 278–289. https://doi.org/10.1016/j.jmapro.2016.03.014
- 26. Iwaszko J. New trends in friction stir processing: rapid cooling—A review. Transactions of the Indian Institute of Metals, 2022, 75, 1681–1693. https:// doi.org/10.1007/s12666-022-02552-2
- 27. Langari J., Kolahan F. The effect of friction stir welding parameters on the microstructure, defects, and mechanical properties of AA7075-T651 joints. Scientia Iranica, 2019, 26(4), 2418–2430. https://doi.org/10.24200/sci.2018.5700.1434
- 28. Hatamleh O., Lyons J., Forman R.. Laser and shot peening effects on fatigue crack growth in friction stir welded 7075-T7351 aluminum alloy joints. International Journal of Fatigue, 2007, 29(3), 421–434. https://doi.org/10.1016/j.ijfatigue.2006.05.007
- 29. Bayazid S.M., Farhangi H., Asgharzadeh H., Radan L., Ghahramani A., Mirhaji A. Effect of cyclic solution treatment on microstructure and mechanical properties of friction stir welded 7075 Al alloy. Materials Science and Engineering A, 2016, 649, 293–300. https://doi.org/10.1016/j.msea.2015.10.010
- Kosturek R., Torzewski J., Wachowski M., Śnieżek L. Effect of welding parameters on mechanical properties and microstructure of friction stir welded AA7075-T651 aluminum alloy butt joints. Materials, 2022, 15(17), 5950. https://doi.org/10.3390/ma15175950
- 31. Manikandan P., Prabhu T.A., Manwatkar S.K., Rao G.S., Murty S.V.S.N., Sivakumar D., Pant B., Mohan M. Tensile and fracture properties of aluminium alloy AA2219-T87 friction stir weld joints for aerospace applications. Metallurgical and Materials Transactions A, 2021, 52(9), 3759–76. https://doi.org/10.1007/s11661-021-06337-y